Test Curves

We use the curves as on page 1 of Lecture 22.

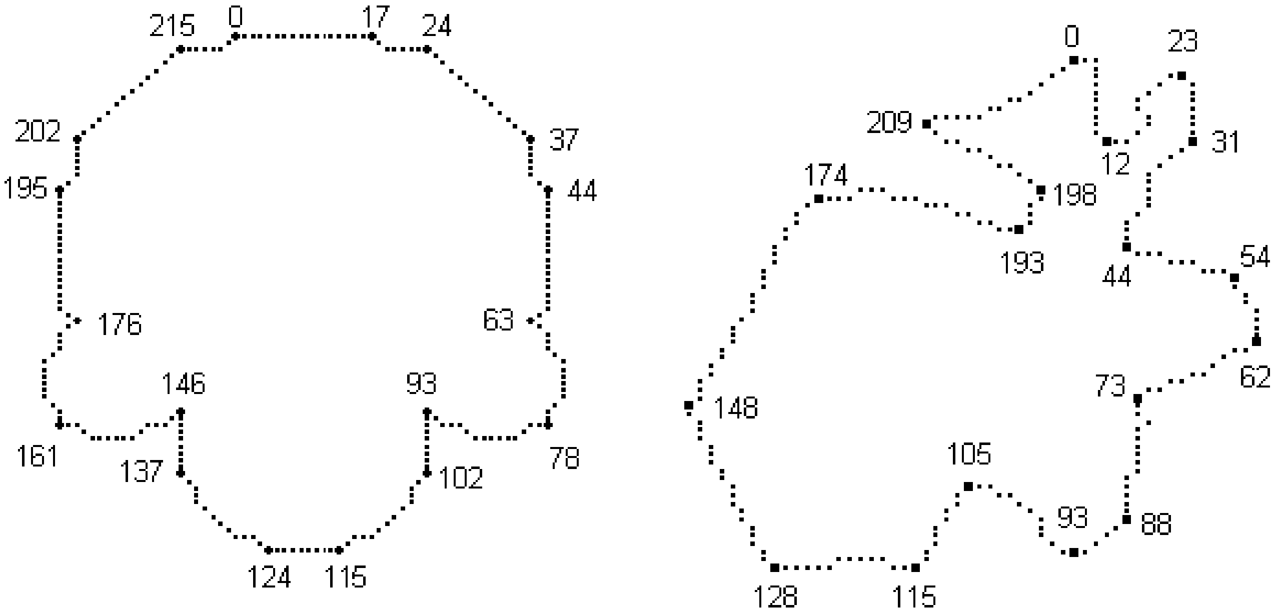

But note that the pixels are counted here starting with zero. These 8-curves can be used for calculating curvature estimates, and for detecting corners based on these estimates. Then we compare detected corners with visually perceived shapes. Note that this is a subjective approach, leading to “weak” judgments such as “as expected”, “not corresponding to visual shape”, etc.

The curve on the left is symmetric; the symmetry of detected corners could be (extending the performance evaluation as given here) measured by a quantitative measure.

M. Marji provided in 2003 the results shown on pages 2-7 as a contribution to the textbook.

RJ1973

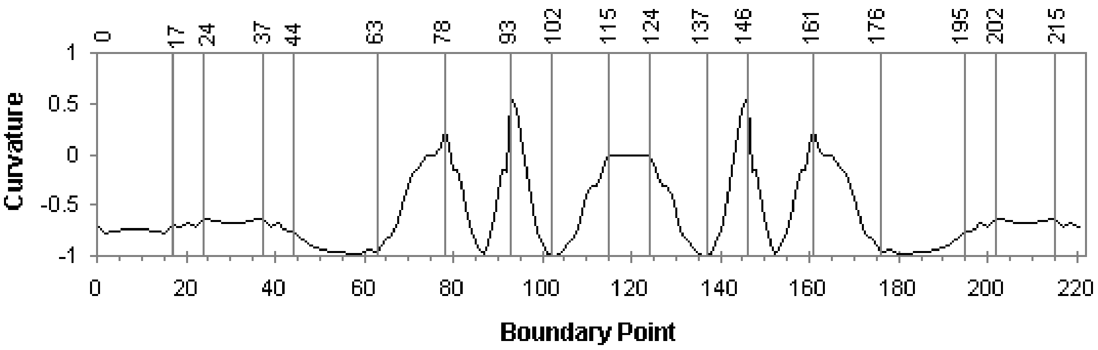

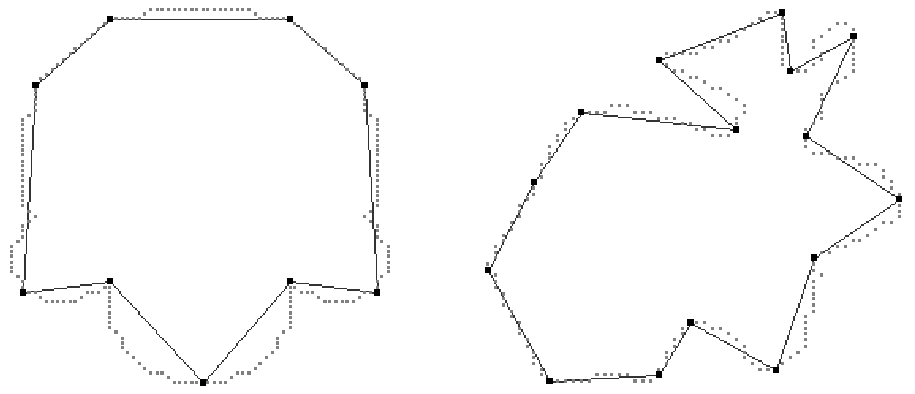

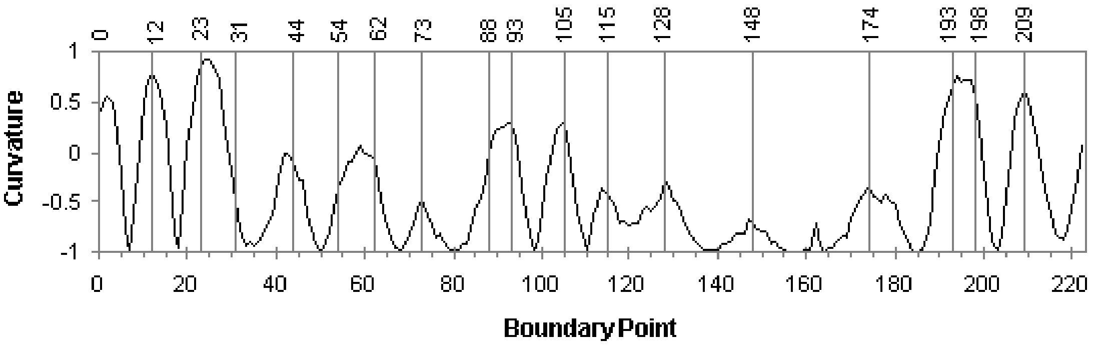

We use $a = 0{\cdot}1$. There is a "plateau" between 115 and 124 in the upper diagram for the symmetric curve, and the original algorithm would take all the points in this plateau as "corners". Instead we selected in such a case the central point only.

FD1977

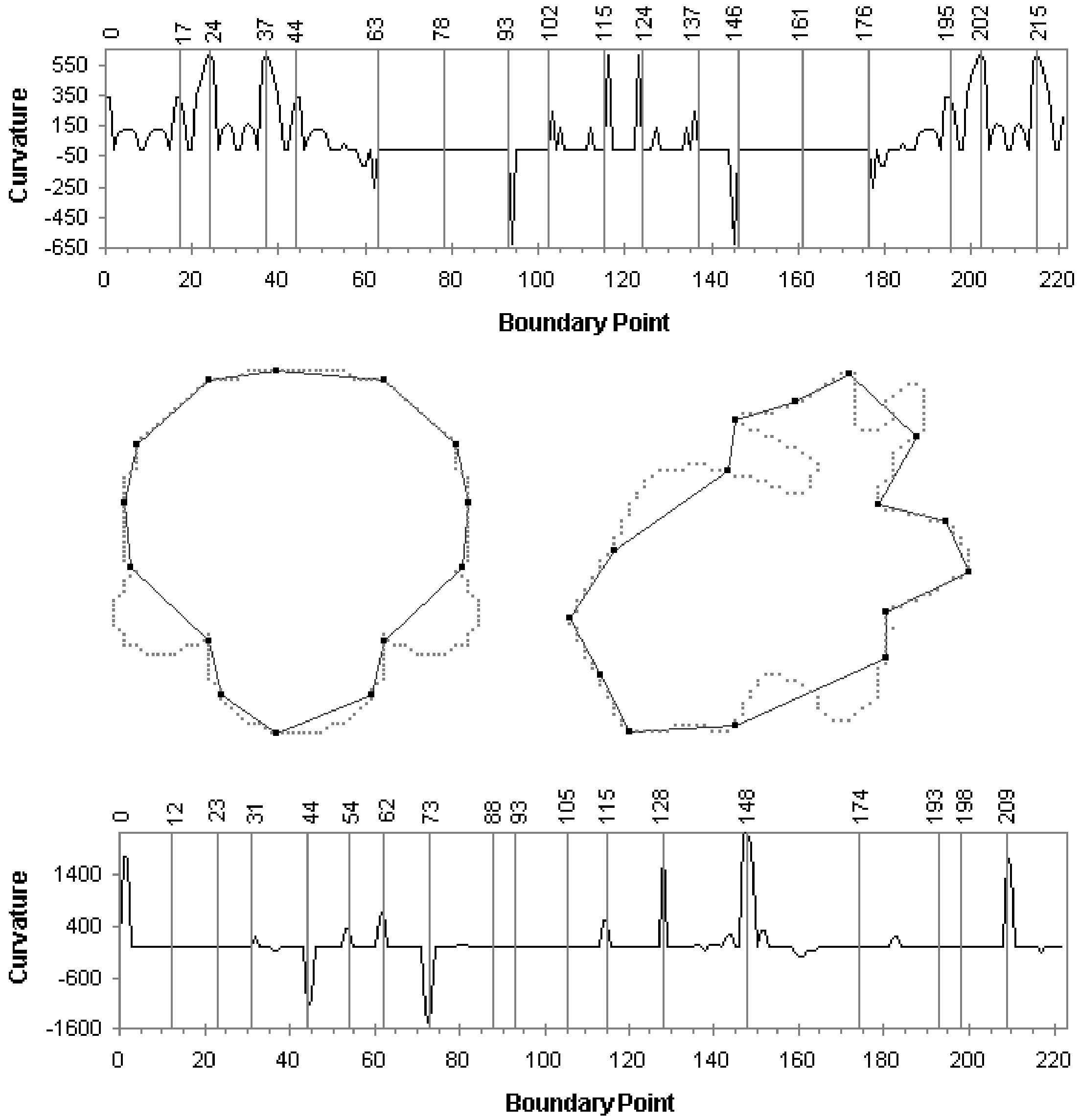

We use $k = 9$. The curvature estimate *is* symmetric for the symmetric curve. However, the criteria used in the original algorithm for detecting corners from this measure (no corner detected in [63-93] and [146-176]) may produce non-symmetric corners. [Symmetric results could be obtained if the criterion is changed to: Select point p_i as corner if $S(p_i) > S(p_j)$ for all points p_j that are within distance k from p_i.]

BT1987

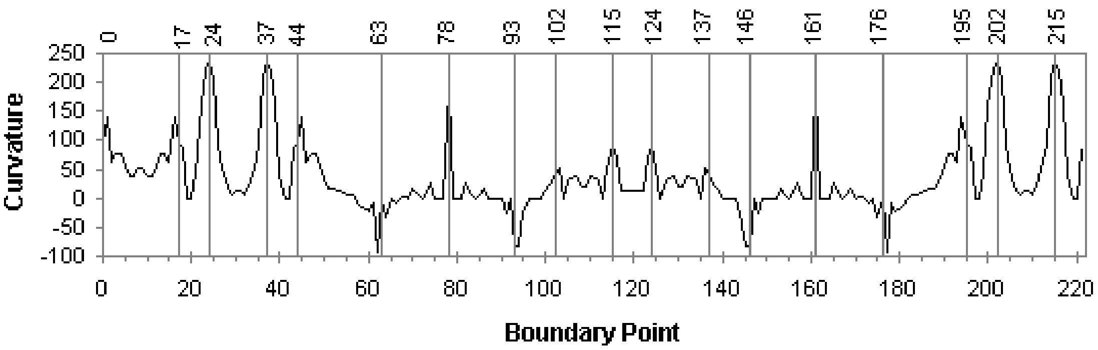

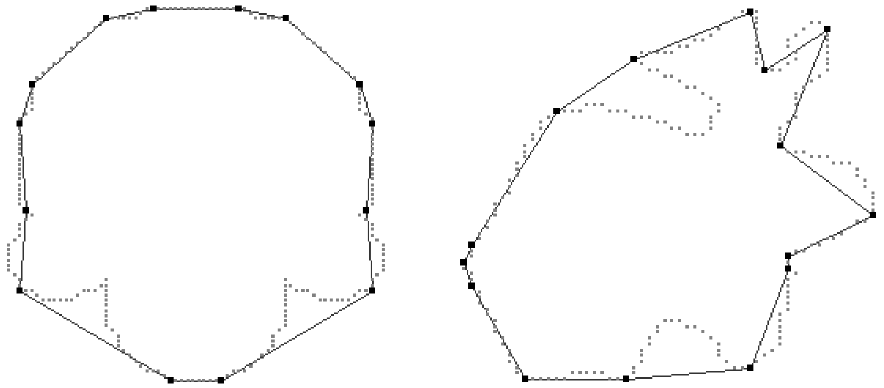

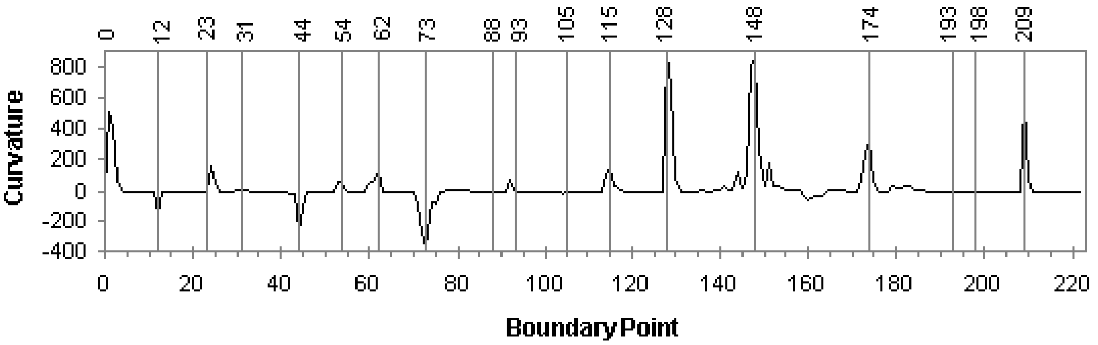

We take $k_L = 9$ (=5 for “rabbit”), $k_U = 14$ (=11), Max_corners=14 (=15), $b = 0{\cdot}1$ (=0·1), i.e. the same number of corners as detected by **FD1977**. The original algorithm **BT1987** reports the most significant corners first, and this is basically the reason for improved results.

M2003

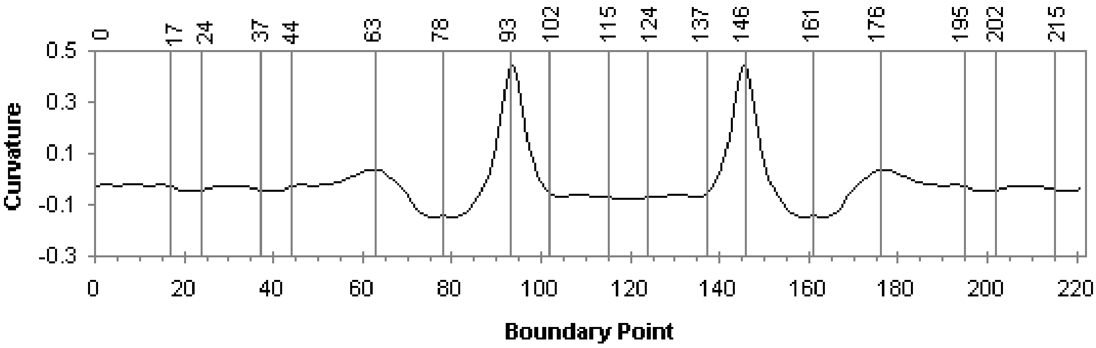

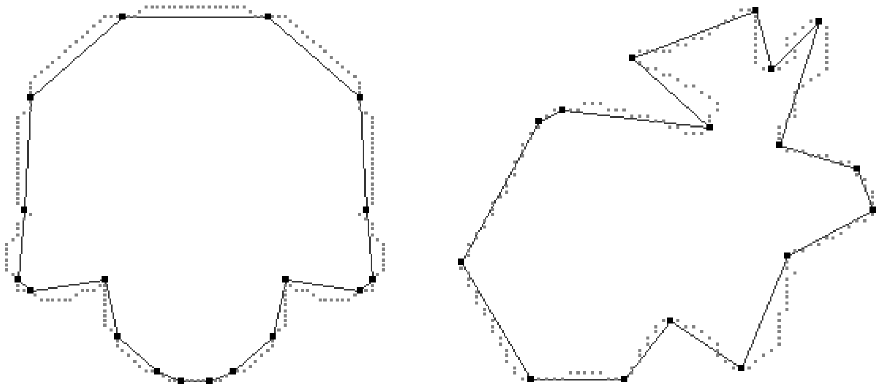

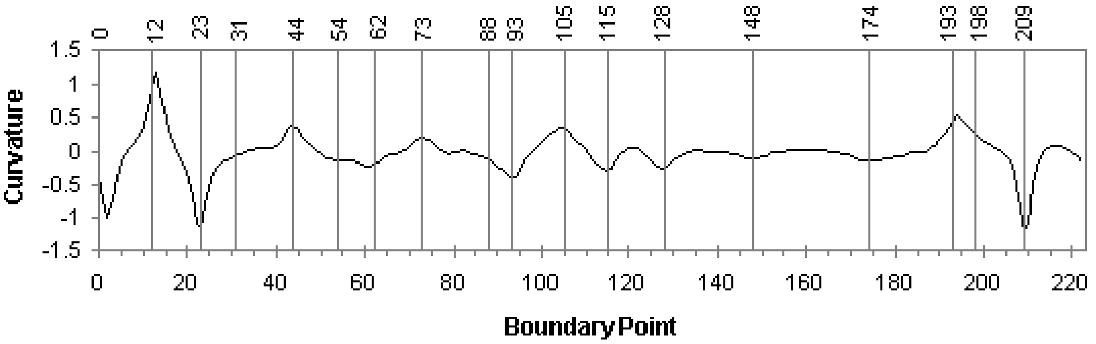

We take $k = 10$ for the symmetric curve, $k = 6$ for the “rabbit”, and threshold 0.08. Subsequences of detected corners may be “close to collinear”, and this can be avoided by applying a final collinearity test.

HK2003

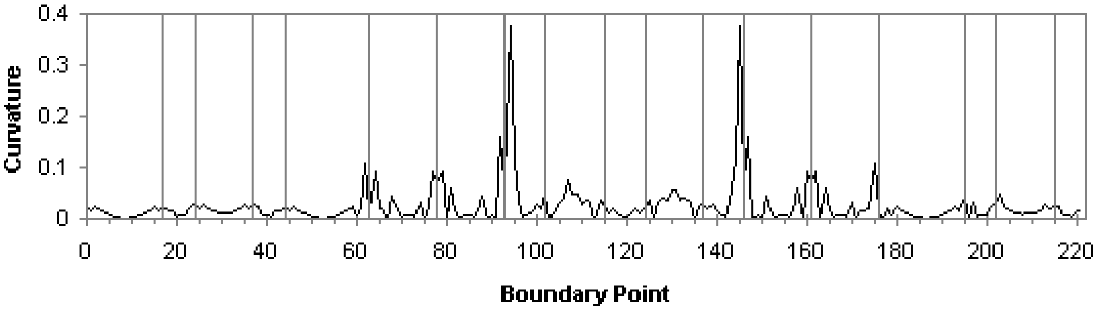

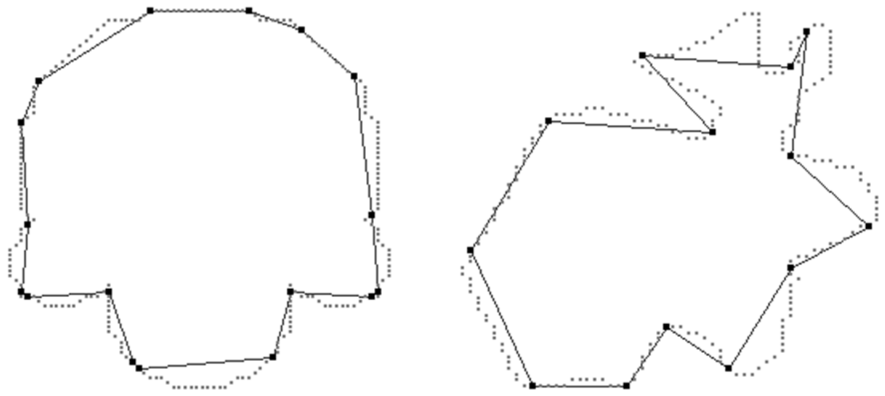

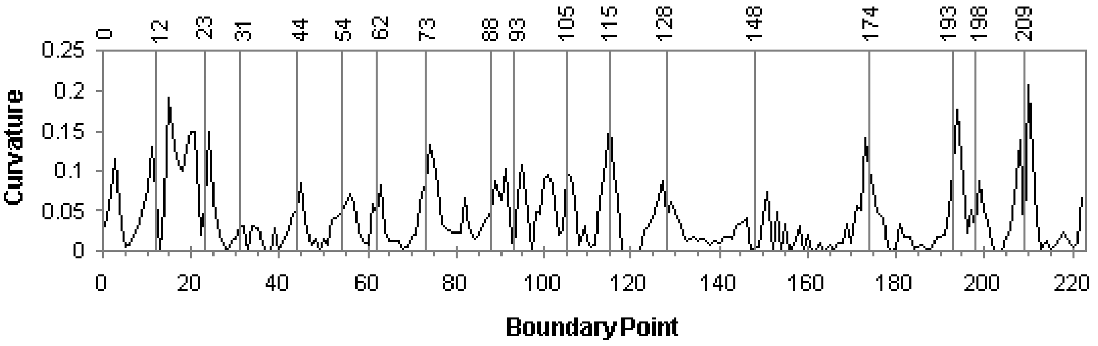

Extending the original algorithm, corner points are extracted from the curvature estimate as follows: if the DSS lines for point p_i span b pixels backwards and f pixels forward, then p_i is a "corner" if its curvature is greater than, or equal to the curvature of all the points in $p_{i-b}, \ldots, p_{i+f}$.

The following figures show the backward and forward extents (in pixels) of the DSSs for each curve pixel. Note that **HK2003** is not symmetric due to the asymmetry of detected DSSs.

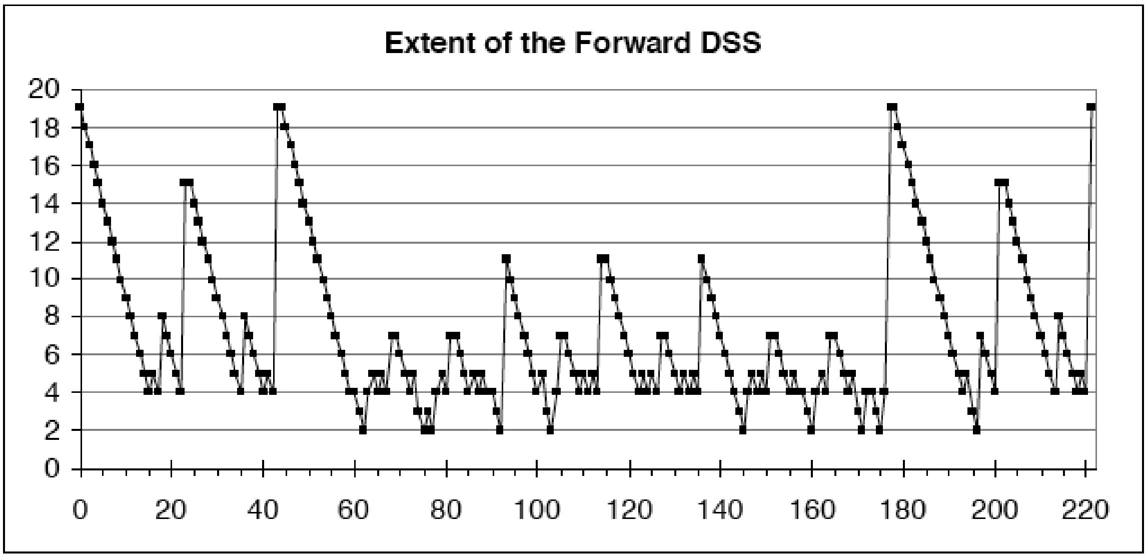

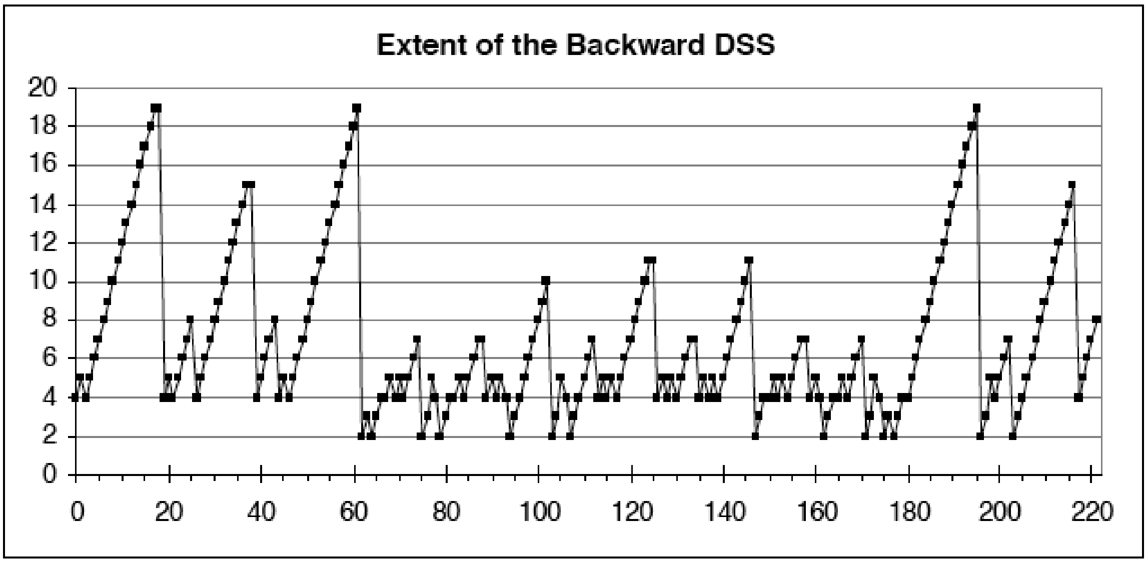

Multigrid Curvature Evaluation

We compare **CMT2001** (as Method 1) and **HK2003** (as Method 2) on two digital circles with about the same radius:

- Disk 1: $\mathbf{x^2 + y^2 \leq r^2}$
- Disk 2: $\mathbf{x^2 + y^2 \leq r^2 + r}$

These disks are digitized (Gauss digitization). The 4-borders are traced by 8-curves, defining digital circles. DSS approximation may produce very short DSSs for Disk 1:

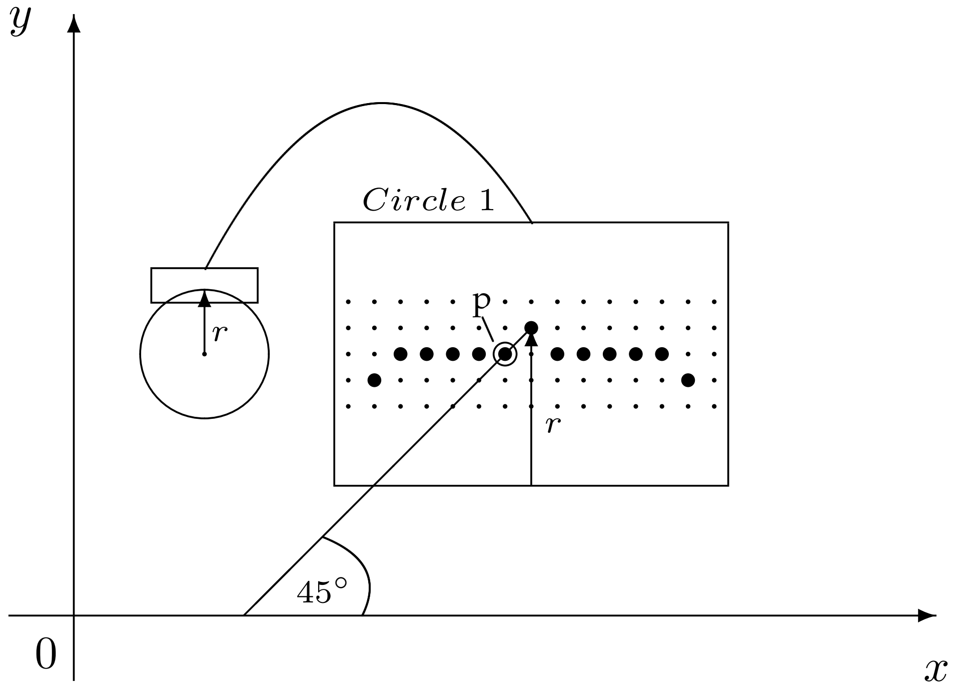

Assume r in the interval $[1, ..., 1040]$ and grid constant $\theta = 1$. We estimate the curvature for all pixels of these digital circles, and determine the mean and the maximum error. Let $\max_r$ be the maximum and mean_r the mean error of the curvature estimates for all grid points on these digital circles.

Values are shown in the diagrams in steps of 10. The values are determined as sliding means as $\frac{1}{39}\sum_{i=-19}^{19} mean_{r+i}$ for the mean error, and $\frac{1}{79}\sum_{i=-39}^{39} max_{r+i}$ for the maximum error.

Mean errors of both methods, for both digital circles. The bold lines are for Disk 1, and the thin lines for Disk 2:

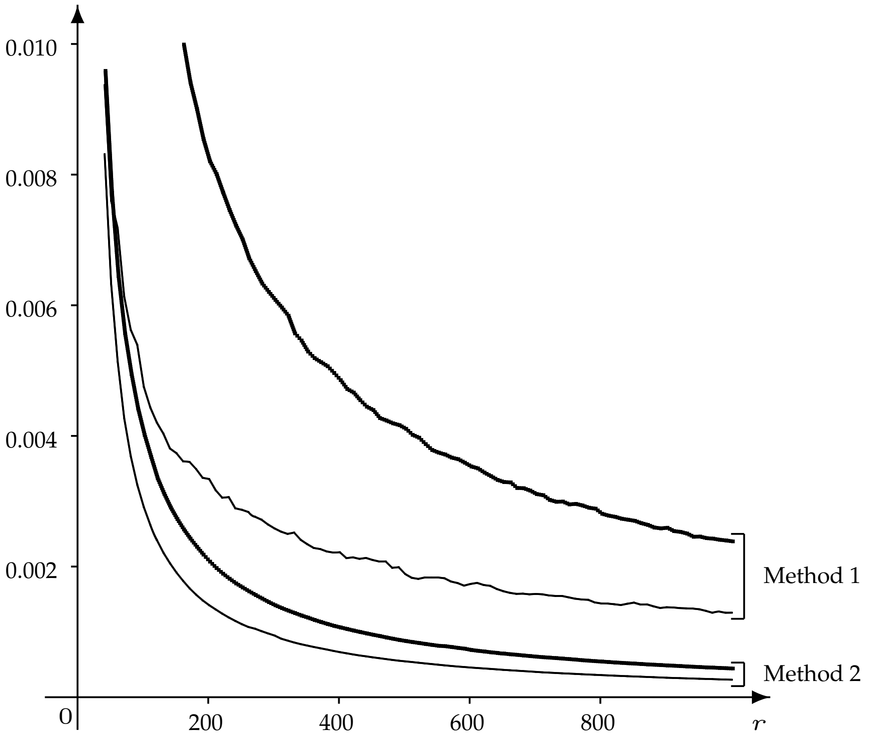

The diagram indicates convergence to the true curvature value (if r increases) for both methods, and a faster convergence for **HK2003** compared to **CMT2001**.

Both methods apply DSS approximations without a-priori length limitation of calculated DSSs. In this sense they are *global methods*. A length limitation will specify a *local method*:

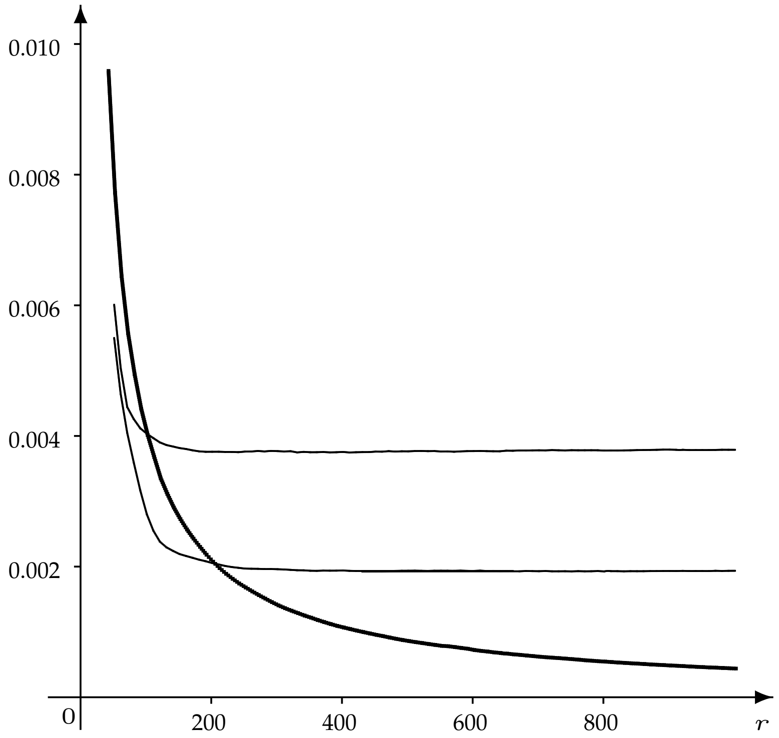

Mean errors of **HK2003** for Disk 1: bold line for the original global method (which has no length limitation for calculated DSSs), followed by lines for derived local methods defined by length limitations $k = 7$ or $k = 5$ (from bottom to top, in the order as on the right of the figure).

The local methods also show convergence, but to incorrect values.

CMT2001 (top) and **HK2003** (bottom); mean errors for Disk 1 (dotted line), maximum errors for Disk 2 (thin line), and mean errors for Disk 2 (bold line) .

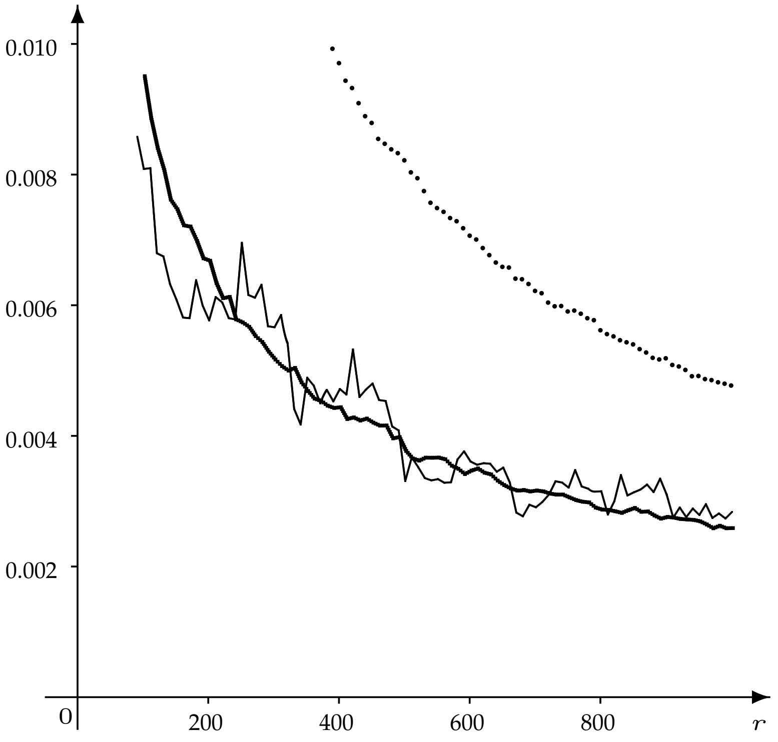

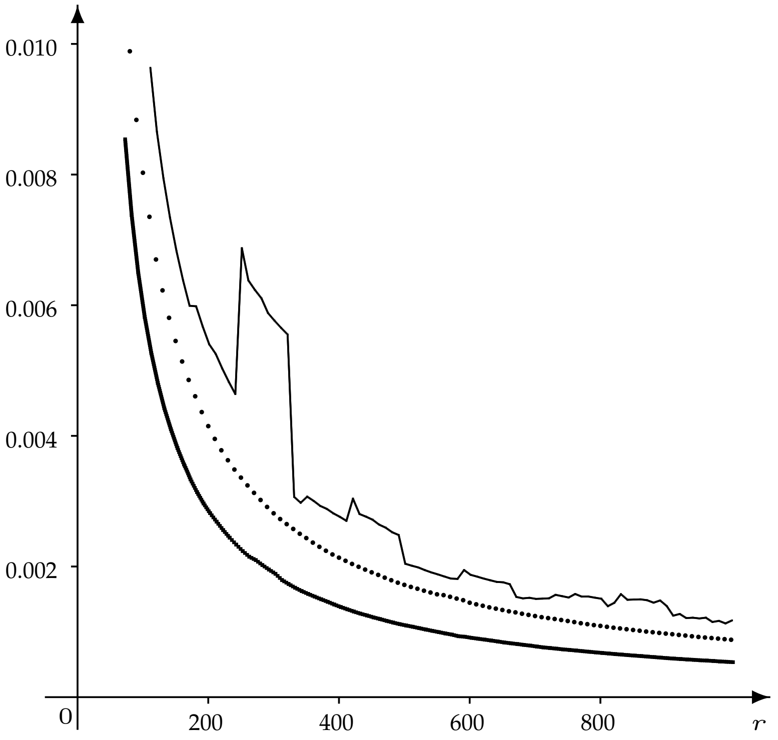

Coursework

Related material in textbook: Section 10.4.3.

A.24. [7 marks] The equation of an *hyperbolic spiral* in polar coordinates is $\gamma(\varphi) = a/\varphi$, for a fixed real $a > 0$. The curve consists of two branches (developing "towards the right" or "towards the left") which are mirror-symmetric to the y-axis:

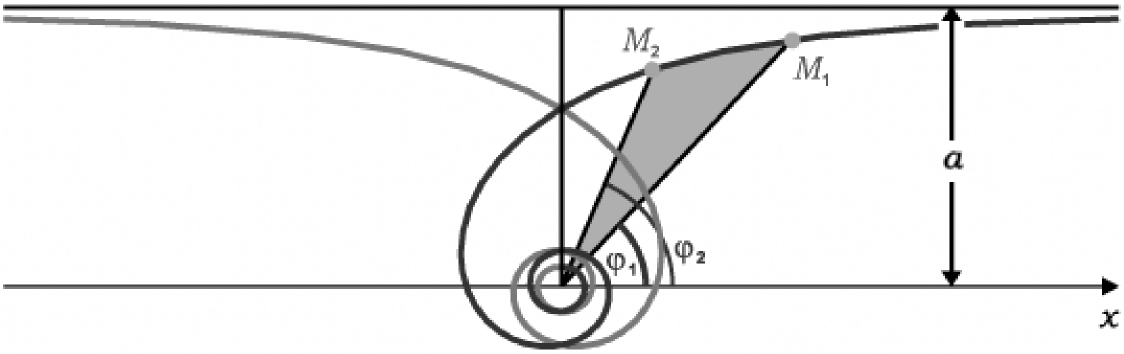

The function is one-to-one; different angles φ_1 or φ_2 define different points M_1 or M_2 on the hyperbolic spiral. The curvature at $\gamma(\varphi)$ is equal to

$$\kappa(\varphi) = \frac{a}{\varphi}\left(\frac{\sqrt{1+\varphi^2}}{\varphi}\right)^3$$

.

Evaluate two different curvature estimators on grid-intersection digitizations of this curve by following the provided example for **CMT2001** and **HK2003** and digital circles. (The logarithmic spiral and the Archimedes spiral are two alternative options; it is sufficient to consider digitizations of one of these curves.)